Health Science Reports

WILEY

Health Science Reports
Open Access

ORIGINAL RESEARCH OPEN ACCESS

Identification of Serum-Derived CricRNA Diagnostic Panel and Revealing Their Regulatory Mechanisms in HCV-HCC: A Cross-Sectional Study

Yasmeen Ishaq[1] | Bisma Rauff[2] | Badr Alzahrani[3] | Hassnain Javed[4] | Aqsa Ikram[1]

[1]Institute of Molecular Biology and Biotechnology (IMBB), University of Lahore (UOL), Lahore, Pakistan | [2]Department of Biomedical Engineering, UET Lahore, Narowal campus, Narowal, Pakistan | [3]Department of Clinical Laboratory Sciences, College of Applied Medical Sciences, Jouf University, Sakaka, Saudi Arabia | [4]Provincial Public Health Reference Lab Lahore, Punjab AIDS Control Program, Lahore, Pakistan

Correspondence: Aqsa Ikram (aqsa.ikram@imbb.uol.edu.pk)

Received: 19 July 2024 | **Revised:** 19 November 2024 | **Accepted:** 25 November 2024

Funding: This research was supported by the Deputyship for Research & Innovation, Ministry of Education in Saudi Arabia for funding this research through project number 223202.

Keywords: cricRNAs panel | HCV | hepatocellular carcinoma | inflammatory responses | tumor microenvironment

ABSTRACT

Aims and Objectives: Hepatitis C virus (HCV) infection is a significant risk factor for the development of hepatocellular carcinoma (HCC). Serum-derived circular RNAs (circRNAs) play several crucial roles in HCV and HCC. They represent a promising area of research for improving the diagnosis and understanding the mechanisms of HCV-HCC. This study aims to identify a serum-derived circular RNA (circRNA) diagnostic panel for HCV-HCC and to elucidate the regulatory mechanisms underlying their role in cancer progression.

Methods: In this study, data mining and in silico analysis were conducted to identify the role of circular RNAs (hsa_circ_0003288, circ-RNF13, hsa_circ_0004277, circANRIL, circUHRF1, hsa_circ_103047) and their associated biomarkers (IL-6 and NF-κB) in HCV-HCC pathogenesis. Additionally, RT-PCR was performed to assess their expression levels across different study groups (G0 = control, G1 = HCV, G2 = HCC, and G3 = HCV-induced HCC).

Results: The expression levels of circular RNAs, including hsa_circ_0003288, circ-RNF13, hsa_circ_0004277, circANRIL, circUHRF1, and hsa_circ_103047, as well as the biomarkers IL-6 and NF-κB, were significantly elevated in the G3 group compared to the G0 group. ROC analysis also revealed significantly different expression rates for G3 group and G0 group.

Conclusion: The data revealed that cricRNAs panel (hsa_circ_0003288, circ-RNF13, circANRIL, circUHRF1, and hsa_circ_103047) could serve as a diagnostic biomarker and therapeutic target for HCV-induced HCC.

1 | Introduction

Cancer is a leading cause of death worldwide, affecting millions of people each year across all regions and demographics [1]. Hepatocellular carcinoma (HCC), accounting for approximately 90% of primary liver cancers, is a significant contributor to this burden [2]. It is caused by several variable etiological factors, like alcohol, HBV, HCV, aflatoxins, and metabolic diseases [3–5]. Hepatitis virus (HCV) belongs to the *Flaviviridae* family. It is a positive-sense single stranded RNA enveloped virus [6, 7]. The acute phase of HCV infection begins following an incubation period of 2 to 12 weeks within the host cell [8]. In most cases, acute infection resolves naturally; however, if it fails to clear on its own, it progresses into chronic hepatitis C (CHC) [9]. Characteristics of CHC are constant hepatic inflammation, the development of hepatic fibrosis, and cirrhosis [10]. The

molecular mechanisms behind HCC progression may vary based on various factors, and hence, several processes may be involved [5, 11].

Circular RNAs (cricRNAs) are a type of noncoding RNA [12]. It plays an important regulatory role in the pathological and biological mechanisms of several diseases [13]. Interestingly, several studies have revealed that circRNAs are closely associated with various tumors, including hepatocellular carcinoma (HCC) [13]. They play a critical role in the development and progression of tumors via the ceRNA mechanism [14]. Various studies suggested that circRNAs hold great potential as diagnostic markers and therapeutic targets for HCC [15]. However, numerous unidentified circRNAs and their associated mRNAs remain to be explored [14]. Recent studies have also reported the role of circRNAs in immune responses [16], including cancer immune evasion [17]. Some circRNAs can activate immunocytes, promoting their fight against tumor [18]. CircRNAs also play a crucial role in regulating the occurrence and progression of HCC by targeting various miRNAs and protein-coding genes involved in processes such as autophagy, tumor cell division, angiogenesis, epithelial-mesenchymal transition, metastasis, and apoptosis [19]. Functionally, circRNAs can affect various components of the tumor microenvironment, specifically at the tumor–immune synapse in HCC [16, 20]. Particularly, it has been discovered that circRNAs regulate the expression of immunological checkpoint regulator molecules in cancer cells [20].

It is worth noting that previous studies have highlighted the roles of circRNAs such as hsa_circ_0003288 [21], circ-RNF13 (hsa_circ_0067717) [22], hsa_circ_0004277 [23], circANRIL (hsa_circ_0008574) [24], circUHRF1 (hsa_circ_0048677) [25], and hsa_circ_103047 [26] in various diseases. However, no study to date has investigated their role in the development of HCV-induced HCC. In this study, we aim to identify a serum-derived circRNA diagnostic panel cricRNAs, including hsa_circ_0003288, *circ-RNF13*, hsa_circ_0004277, circANRIL, circUHRF1 and hsa_circ_103047 for HCV-associated HCC and investigate the regulatory mechanisms by which these circRNAs contribute to cancer progression. In this study, we compare the relative expression levels of these six circRNAs across four groups: G1 (HCV patients), G2 (HCC patients with unknown etiology), G3 (HCC-HCV patients), and G0 (healthy controls). Additionally, we aim to assess the correlation of these circRNAs with immune-related biomarkers and evaluate their diagnostic potential. By elucidating the diagnostic value and functional roles of circRNAs in HCV-HCC, this research seeks to provide new insights into early detection and therapeutic targets for this aggressive liver cancer.

2 | Methods

2.1 | Sample Collection

The present study included 100 Individuals, divided into four groups: (1) G0 group: 20 healthy individuals, (2) G1 group: 20 HCV-infected patients, (3) G2 group: 20 HCC patients (negative for HCV/HBV/alcoholic-induced cancer), and (4) G3 group: 40 HCV-induced HCC patients. Blood samples from patients from different cancer-hospitals in Pakistan were collected. 5 mL of peripheral blood were taken and preserved at −80°C in EDTA-vacutainers. Informed consents were taken from all participants. The Research Ethics Committee of the University of Lahore (REC-UOL) approved the present study. For the present study CONSORT guidelines and guidelines by Assel et al., 2018 were followed for proper analysis, reporting, and interpretation of clinical research [27, 28].

2.2 | Inclusion and Exclusion Criteria

All participants in this study had to be older than 18 years. Study participants included healthy people with normal liver function, no history of liver disease, and generally good health with no significant kidney, heart, lung, or other essential organ disease. Included were HCV patients who tested positive for circulating anti-HCV-antibodies. Patients diagnosed with HCC and HCV-induced HCC have at least two imaging techniques (i.e., hepatic ultrasound along with MRI or CT, or both), and were in an advanced stage of the disease. Patients with a history other than HCV-infection or HCC induced by HBV or alcoholism or with a history of other types of cancer were excluded from this study.

2.3 | HCV Antibodies Testing

HCV antibodies test was performed for quantitative detection of antibodies in serum with the help of COBAS AmpliPrep/COBAS TaqMan HCV Quantitative Tests, v2.0 on the cobas 6800 system (Roche Diagnostics, Mannheim, Germany).

2.4 | RNA Extraction and cDNA Synthesis

Total RNA was extracted from all samples with the help of Quick-RNA MiniPrep Plus (ZYMO RESEARCH Cat # R1057, USA), and its quantity and quality were calculated with the help of the Qubit 4 Fluorometer (Thermo Fisher Scientific, USA) by using Qubit RNA HS Assay Kit Catalog # Q32852). The RevertAid First Strand cDNA Synthesis Kit (Thermo Scientific #K1622) was used to make cDNA from total RNA on the Applied Biosystems Veriti 96-Well Thermal Cycler Cat# 4375786).

2.5 | RT-PCR Amplification

RT-PCR of the circRNAs including hsa_circ_0003288, *circ-RNF13*, hsa_circ_0004277, circANRIL, circUHRF1, hsa_circ_103047, and immune-related biomarkers IL-6 and NF-κB was performed on the QIAGEN Rotor-Gene Q 5 PLEX HRM Real-Time PCR machine using Maxima SYBR Green/ROX qPCR Master Mix (2X) (Thermo Scientific #K0221). As an internal reference gene,

glyceraldehyde-3-phosphate dehydrogenase (GAPDH) was used. Sequences of primers are the following:

Hsa_circ_103047	F 5′-CACTGACTTGCCACTCCTTTG-3′
	R 5′-GTCTGTTAGGTGGATGCTTTGT-3′
Hsa_circ_0004277	F 5-CACTTACAAGGCTTCCAC-3′
	R 5′-CTTACTCAGCTCTGCTCC-3′
CircUHRF1	F 5′-GCTATGAGGATGATGTGGGAT-3′
	R 5′-CAGAGTCTGTTCACGTCGTCC-3′
CircANRIL	F 5′-GCTGGGATTACAGGTGTGAGACACC-3′
	R 5′-GAATCAGAATGAGGCTTATTCTTCTCATC-3′
Circ-RNF13	F 5′-GCAGACATCGAAGCCAAACA-3′
	R 5′-ACTGCTGTTTGGCTTCGATG -3′
Hsa_circ_0003288	F 5′-AAAGGGGTGCTTTCCAGACA-3′
	R 5′-GCCAATCTTATTCGTCCGGG-3′
IL-6	F 5′-CTGCGATGGAGTCAGAGGAA-3′
	R 5′-TTCTCTTTCGTTCCCGGTGG-3′
NF-κB	F 5′-GCACCCTGACCTTGCCTATT-3′
	R 5′-CTGCTTGGCGGATTAGCTCT-3′
GAPDH	F 5′-CGACCACTTTGTCAAGCTCA-3′
	R 5′-AGG GGT CTA CAT GGC AAC TG-3′

2.6 | Data Analysis

Relative expression levels hsa_circ_0003288, circ-RNF13, hsa_circ_0004277, circANRIL, circUHRF1, hsa_circ_103047, *IL-6*, and *NF-κB* were calculated with the help of the $2^{-\Delta\Delta Ct}$ method [29].

2.7 | CricRNA-miRNA-mRNA Network Construction

We used CircNetVis (https://www.meb.ki.se/shiny/truvu/CircNetVis/) as a specialized bioinformatics website to visualize cricRNAs interaction networks [30]. TargetScan was used to find out the target genes of the selected miRNAs [31]. Cytoscape (version 3.10.1) was used to construct the cricRNA-miRNA-mRNA network [32].

2.8 | Statistics Analysis

Statistical analysis was performed with the help of GraphPad Prism 8.0.2 and represented as mean ± SD. Statistical comparisons of data were found by one-way analysis of variance (ANOVA), either the Kruskal-Wallis H test or Tukey post-hoc analyses. Spearman's correlation analysis was used to evaluate relationships among candidate cricRNAs and immune-related biomarkers. To evaluate the sensitivity and specificity of the controls and HCV-induced HCC cases, the area under the curve (AUC) was calculated, and a receiver operating characteristic (ROC) curve was created ($p < 0.05$). All statistical tests performed in this study were two-tailed, and statistically, a $p \leq 0.05$ was considered significant. All the statistical analysis were performed according to the SAMPL guidelines [33].

3 | Results

The demographical features of G0 group (healthy individuals), G1 group (HCV patients), G2 group (HCC patients with unknown etiology factor), and G3 group (HCV induced HCC) are mentioned in Table 1.

3.1 | Relative Expression of CricRNAs and Biomarkers

The relative expression levels of hsa_cric_0003288, cric-RNF13, hsa_cric_0004277, cric-ANRIL, cricuHRF1, hsa_cric_103047, and biomarkers *IL-6* and *NF-κB* among the G0, G1, G2, and G3 groups were compared by Tukey's multiple comparison test. Expression levels of all cricRNAs including hsa_cric_0003288, cric-RNF13, hsa_cric_0004277, cric-ANRIL, cricuHRF1, hsa_cric_103047, and biomarkers like *IL-6*, and *NF-κB*, were found significantly upregulated in the G3 group ($p = 0.03$, $p = 0.02$, $p = 0.01$, $p = 0.001$, $p = 0.01$, $p = 0.03$, $p = 0.05$, and $p = 0.04$, respectively) and the G2 group ($p = 0.005$, $p = 0.02$ and $p = 0.002$, $p = 0.0002$, $p = 0.009$, $p = 0.005$, $p = 0.03$, and $p = 0.02$, respectively) as compared with the G0 group. The expression levels of hsa_cric_0003288, cric-RNF13, hsa_cric_0004277, cric-ANRIL, cricuHRF1, hsa_cric_103047, and NF-κB were also significantly upregulated in the G3 group ($p = 0.03$, $p = 0.02$, $p = 0.03$, $p = 0.02$, $p = 0.02$, $p = 0.05$, and $p = 0.04$, respectively) and the G2 group ($p = 0.005$, $p = 0.03$, $p = 0.01$, $p = 0.01$, $p = 0.02$, $p = 0.01$, and $p = 0.03$, respectively) as compared with the G1 group. However, no significant

TABLE 1 | Demographic features of the study groups.

Variables	G0 group (Control) ($n = 20$)	G1 group (HCV) ($n = 20$)	G2 group (HCC) ($n = 20$)	G3 group (HCV-HCC) ($n = 40$)	*p* value
Age	36.7 ± 14.72	47.3 ± 12.99	56.7 ± 10.61	55.4 ± 9.28	0.001
< 50	7 (35.00%)	8 (40.00%)	4 (20.00%)	7 (17.50%)	
≥ 50	13 (65.00%)	12 (60.00%)	16 (80.00%)	33 (82.50%)	
Gender					0.001
Male	8 (40.00%)	11 (55.00%)	15 (75.00%)	29 (27.50%)	
Female	12 (60.00%)	9 (45.00%)	5 (25.00%)	11 (72.50%)	

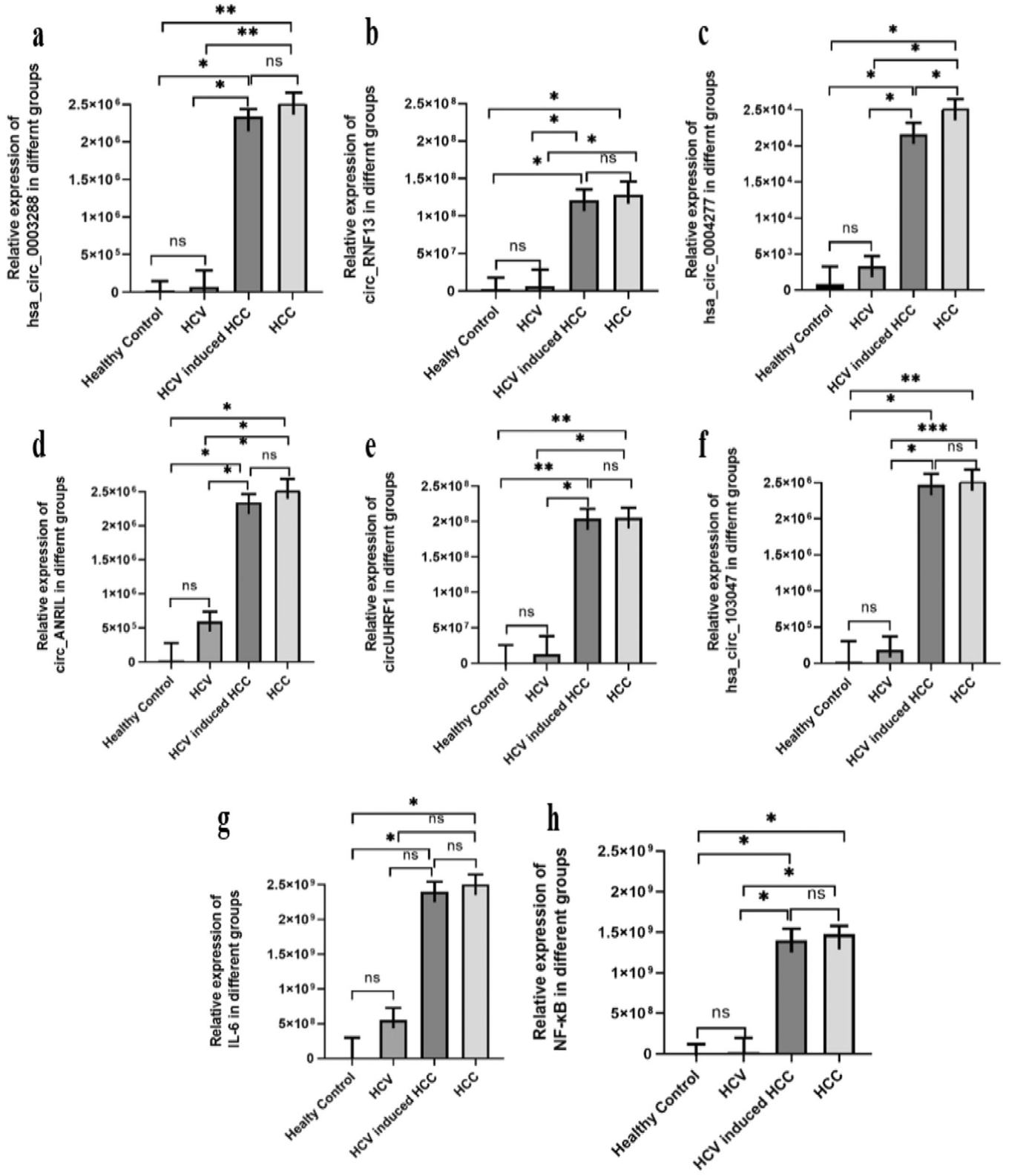

FIGURE 1 | Relative expression of cricRNAs and biomarkers in different study groups. G0 (healthy control), G1 (HCV), G2 (HCC), and G3 (HCV induced HCC). Relative expression of the circRNAs and immune related biomarkers [(a) hsa_cric_0003288, (b) cric-RNF13, (c) hsa_cric_0004277, (d) cric-ANRIL, (e) cricuHRF1, (f) hsa_cric_103047, (g) NF-κB, and (h) IL-6] were calculated by Tukey's multiple comparison test and expression levels of candidates cricRNAs and biomarkers are presented in bar charts. The study groups are represented by the *X* axis, and relative expression of cricRNAs and biomarkers is displayed on the *Y* axis (ns corresponds to $p > 0.05$, * corresponds to significant $p \leq 0.05$, ** corresponds to significant $p \leq 0.01$, and *** corresponds to significant $p \leq 0.001$).

difference was found in the relative expression levels of hsa_cric_0003288, cric-RNF13, hsa_cric_0004277, cric-ANRIL, cricuHRF1, hsa_cric_103047, *IL-6*, and *NF-κB* among the G0 and G1 groups, as well as in the G2 and G3 groups, as shown in Figure 1.

Furthermore, expression levels of hsa_cric_0003288, cric-RNF13, hsa_cric_0004277, cric-ANRIL, cricuHRF1, hsa_cric_103047, NF-κB, and IL-6 in the G0, G1, G2, and G3 groups are also presented in the heatmap. The ΔCt values for each of the cricRNAs and biomarkers were used to generate a heatmap on Microsoft Excel. Low expression is represented by red color, and high expression is represented by green color, as mentioned in Figure 2.

3.2 | CricRNAs Correlation With Immune-Related Biomarkers in Study Groups

In addition, we measured the quantitative levels of immune-related biomarkers (*IL-6* and *NF-κB*) to evaluate their relationship with six validated cricRNAs (hsa_circ_0003288, circ-RNF13, hsa_circ_0004277, circANRIL, circUHRF1, and hsa_circ_103047) using Spearman's correlation analyses. The immune-related biomarkers measured were IL-6 and NF-κB. Cric-RNF13 expression was negatively correlated only with IL-6, and hsa_cric_103047 expression was negatively correlated only with NF-κB in G3 group. In G1 and G2, no significant correlations of cricRNAs with *IL-6* and *NF-κB* were noted, as mentioned in Table 2.

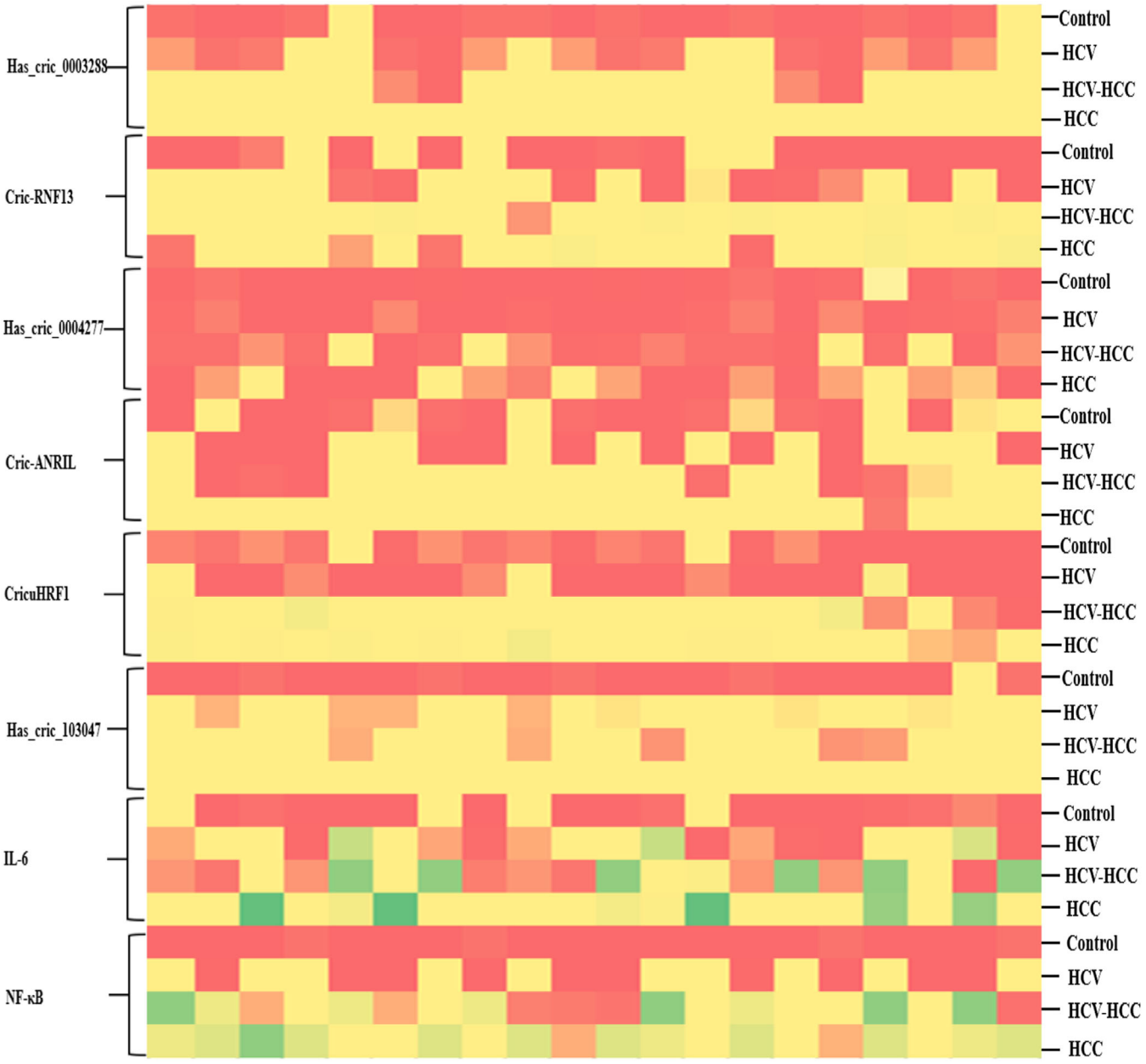

FIGURE 2 | Heatmap of the expression of cricRNAs and immune-related biomarkers in study group G0 (healthy control), G1 (HCV), G2 (HCC), and G3 (HCV induced HCC). The expression levels of cricRNAs and immune-related biomarkers are represented on a red-green scale in the center panel, where the red and green should be interpreted as low and high expression, respectively.

TABLE 2 | Spearman rank correlations of dysregulated cricRNAs and immune-related biomarkers levels in G1, G2 and G3 groups (r/P).

Variables	Hsa_cric_0003288	cric-RNF13	Hsa_cric_0004277	cric-ANRIL	cricUHRF1	Hsa_cric_103047
G1 group (HVC)						
IL-6	$r = -0.05443$ $p = 0.8401$	$r = -0.04217$ $p = 0.8681$	$r = -0.2190$ $p = 0.3825$	$r = 0.2060$ $p = 0.4122$	$r = 0.01935$ $p = 0.9392$	$r = 0.1915$ $p = 0.4887$
NF-κB	$r = 0.2937$ $p = 0.2665$	$r = -0.1322$ $p = 0.5896$	$r = -0.1449$ $p = 0.5661$	$r = 0.01863$ $p = 0.9415$	$r = 0.2346$ $p = 0.3337$	$r = 0.1571$ $p = 0.5712$
G2 group (HCC)						
IL-6	$r = 0.1811$ $p = 0.4977$	$r = -0.2074$ $p = 0.4090$	$r = -0.1239$ $p = 0.6243$	$r = 0.2661$ $p = 0.2857$	$r = 0.2320$ $p = 0.3543$	$r = 0.3358$ $p = 0.2187$
NF-κB	$r = 0.3801$ $p = 0.1456$	$r = 0.01423$ $p = 0.9539$	$r = 0.1615$ $p = 0.5220$	$r = 0.09470$ $p = 0.7086$	$r = 0.2099$ $p = 0.3885$	$r = 0.008532$ $p = 0.9768$
G3 group (HCV-HCC)						
IL-6	$r = 0.1123$ $p = 0.6753$	$r = -0.5352$ $p = 0.0221$	$r = -0.004828$ $p = 0.9848$	$r = 0.1005$ $p = 0.6916$	$r = 0.02425$ $p = 0.9239$	$r = 0.1413$ $p = 0.6107$
NF-κB	$r = 0.08030$ $p = 0.7658$	$r = 0.2371$ $p = 0.3283$	$r = 0.1628$ $p = 0.5186$	$r = -0.1561$ $p = 0.5362$	$r = -0.2972$ $p = 0.2165$	$r = -0.5865$ $p = 0.0240$

3.3 | ROC Analysis

3.3.1 | Diagnostic Potential of CricRNAs and Biomarkers in G1 Group in Comparison with G0 Group

Receiver operating characteristics (ROC) curves were created for candidate cricRNAs and immune biomarkers to differentiate G1 group from G0 group (Figure 3). The area under the ROC curve (AUC) values were 0.8438, 0.6593, 0.6543, 0.5494, 0.64, 0.9333, 0.7716, and 0.8892, corresponding to has_cric_0003288, cric-RNF13, has_cric_0004277, cric-ANRIL, cricuHRF1, has_cric_103047, *IL-6*, and *NF-κB*, respectively. The p-values were statistically significance of has_cric_0003288, cric-RNF13, has_cric_103047, *IL-6*, and *NF-κB* ($p = 0.0009$, $p = 0.0932$, $p < 0.0001$, $p = 0.0054$, and $p = < 0.0001$). However, has_cric_0004277, cric-ANRIL, and cricuHRF1 were not significant ($p = 0.1137$, $p = 0.6127$ and $p = 0.1298$, respectively). All cricRNAs and biomarkers showed sensitivity (ranging from 100% to 61.11%) and specificity (ranging from 100% to 50%) for the identification of G1 group. A combined cricRNA panel and biomarkers' overall sensitivity, specificity, and AUC were 82.52%, 52.45%, and 0.7065, respectively ($p < 0.0001$) (Supporting Information S1: Table S1).

3.3.2 | Diagnostic Potential of CricRNAs and Biomarkers in G2 Group in Comparison with G0 Group

ROC curves were drawn for candidate cricRNAs and immune biomarkers to distinguish G2 group from G0 group (Figure 4). The AUC values were 0.9609, 0.892, 0.6111, 0.9815, 0.945, 0.9822, 0.9506, and 1.00, corresponding to has_cric_0003288, cric-RNF13, has_cric_0004277, cric-ANRIL, cricuHRF1, has_cric_103047, *IL-6*, and *NF-κB*, respectively. The *p*-values were statistically significant for has_cric_0003288, cric-RNF13, cric-ANRIL, cricuHRF1, has_cric_103047, *IL-6*, and *NF-κB* ($p < 0.0001$). However, has_cric_0004277 was not significant ($p = 0.2547$). All cricRNAs and biomarkers showed high sensitivity (ranging from 100% to 84.21%) and specificity (ranging from 100% to 55.56%) for the identification of G2 group. A combined cricRNA panel and biomarkers' overall sensitivity, specificity, and AUC were 76.22%, 82.52%, and 0.8327, respectively ($p < 0.0001$) (Supporting Information S1: Table S1).

3.3.3 | Diagnostic Potential of CricRNAs and Biomarkers in G2 Group in Comparison With G1 Group

ROC curves were drawn for cricRNAs and to distinguish G2 group from G1 group (Figure 5). The AUC values were 0.8828, 0.8227, 0.6019, 0.892, 0.9175, 0.8622, 0.8796, and 0.8006, corresponding to has_cric_0003288, cric-RNF13, has_cric_0004277, cric-ANRIL, cricuHRF1, has_cric_103047, *IL-6*, and *NF-κB*, respectively. The p-values were statistically significant for has_cric_0003288 and *NF-κB* ($p = 0.0002$ and $p = 0.0015$, respectively); cric-RNF13 and has_cric_103047 ($p = 0.0007$); and cric-ANRIL, cricuHRF1, and *IL-6* ($p < 0.0001$). However, has_cric_0004277 was not significant ($p = 0.2965$). All cricRNAs and biomarkers showed sensitivity (ranging from 94.44% to 27.78%) and specificity (ranging from 100% to 53.33%) for the identification of G. A combined cricRNA panel and biomarkers' overall sensitivity, specificity, and AUC were 96.61%, 63.64%, and 0.8200, respectively ($p < 0.0001$) (Supporting Information S1: Table S1).

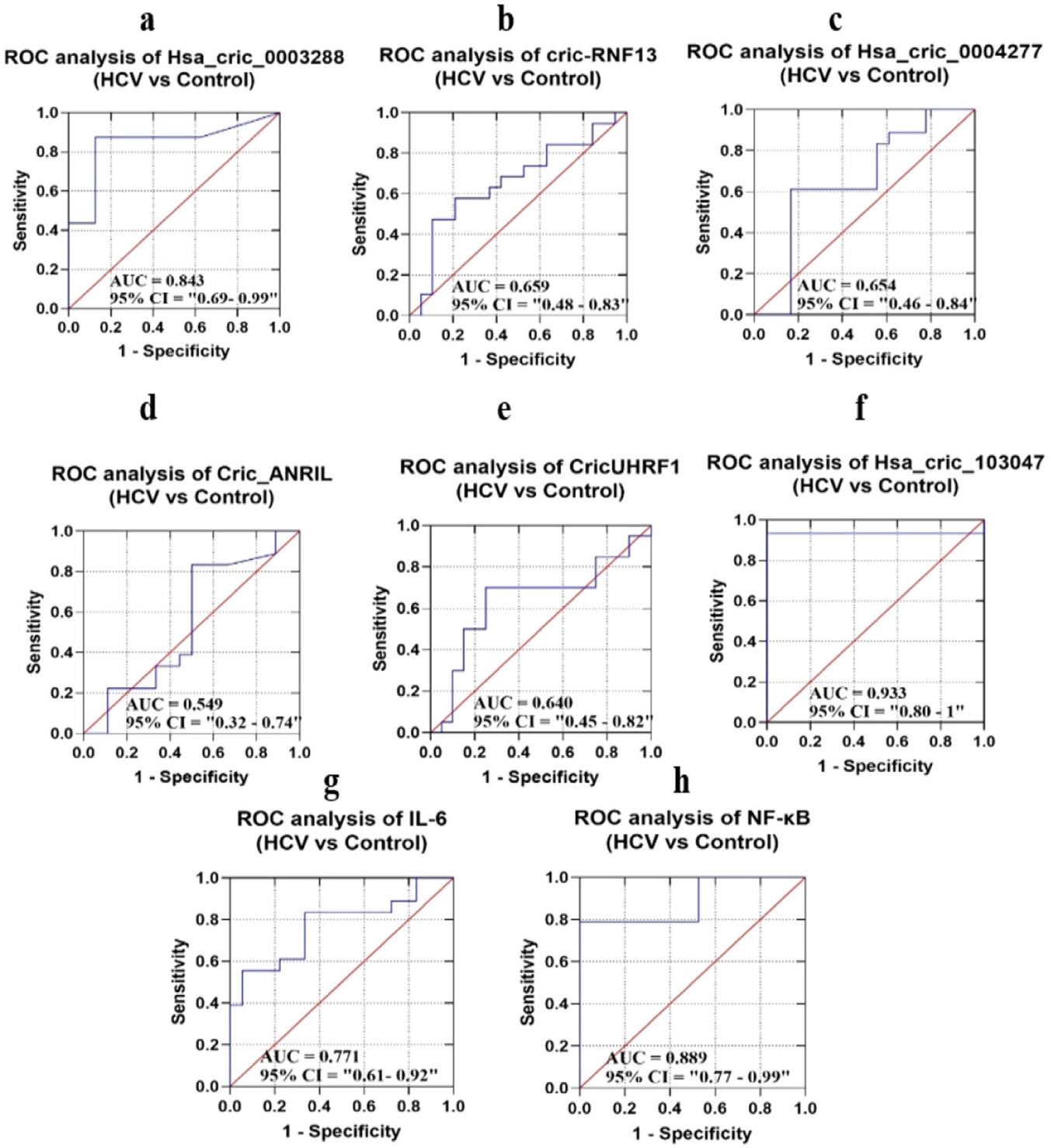

FIGURE 3 | ROC curves and AUC for cricRNAs and immune related biomarkers to distinguish the G1 group (HCV patients) from G0 group (normal controls). The diagnostic potential and AUC of 6 cricRNAs and 2 biomarkers [(a) hsa_cric_0003288, (b) cric-RNF13, (c) hsa_cric_0004277, (d) cric-ANRIL, (e) cricuHRF1, (f) hsa_cric_103047, (g) IL-6, and (h) NF-κB] were estimated.

3.3.4 | Diagnostic Potential of CricRNAs and Biomarkers in G3 Group in Comparison With G0 Group

To discriminate G3 group from G0 group, ROC curve analysis of candidate cricRNAs and immune-related biomarkers was performed (Figure 6). AUC values were 0.9492, 0.8476, 0.821, 0.8148, 0.8775, 0.9689, 0.8796, and 0.9889, corresponding to has_cric_0003288, cric-RNF13, has_cric_0004277, cric-ANRIL, cricuHRF1, has_cric_103047, *IL-6*, and *NF-κB*, respectively. The p value was statistically significant for has_cric_0003288, cricuHRF1, has_cric_103047, *IL-6*, and *NF-κB* ($p < 0.0001$); and cric-RNF13, has_cric_0004277, and cric-ANRIL ($p = 0.0002$, $p = 0.001$, and $p = 0.0013$, respectively). All cricRNAs and biomarkers showed high sensitivity (ranging from 93.33% to 77.7%) and specificity (ranging from 94.74% to 44.44%) for the identification of G3 group. A combined cricRNA panel and biomarkers' overall sensitivity,

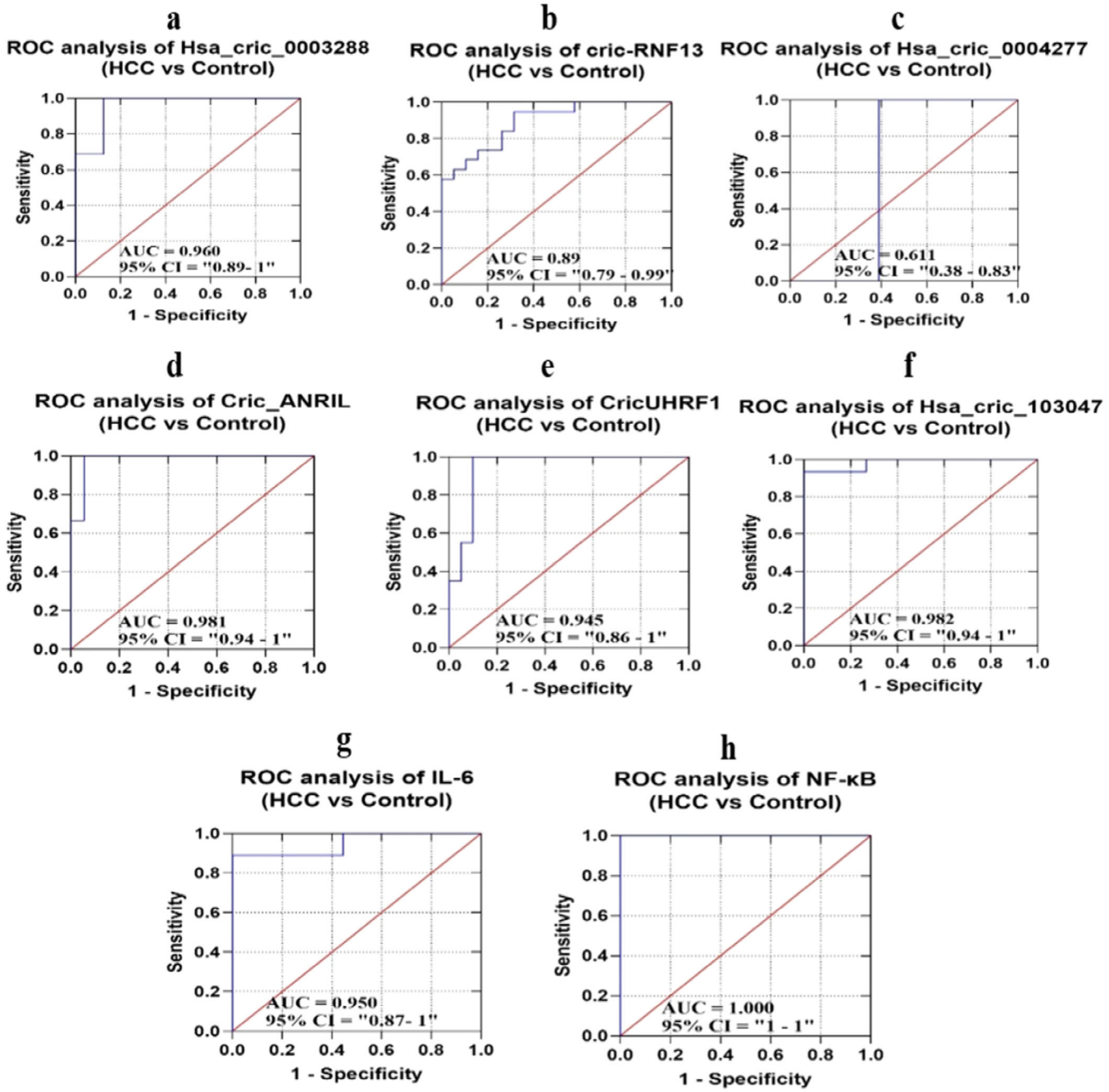

FIGURE 4 | ROC curves and AUC for cricRNAs and immune related biomarkers to differentiate the G2 group (HCC patients) from G0 group (normal controls). The diagnostic potential and AUC of 6 cricRNAs and 2 biomarkers [(a) hsa_cric_0003288, (b) cric-RNF13, (c) hsa_cric_0004277, (d) cric-ANRIL, (e) cricuHRF1, (f) hsa_cric_103047, (g) IL-6, and (h) NF-κB] were estimated.

specificity, and AUC were 72.03%, 74.83%, and 0.8026, respectively ($p < 0.0001$) (Supporting Information S1: Table S1).

3.3.5 | Diagnostic Potential of CricRNAs and Biomarkers in G3 Group in Comparison With G1 Group

To differentiate G3 group from G1 group, ROC curve analysis of cricRNAs and immune-related biomarkers was performed (Figure 7). AUC values were 0.8789, 0.7452, 0.7546, 0.7407, 0.875, 0.6, 0.6358, and 0.7341, corresponding to has_cric_0003288, cric-RNF13, has_cric_0004277, cric-ANRIL, cricuHRF1, has_cric_103047, *IL-6*, and *NF-κB*, respectively. The p value was statistically significant only for has_cric_0003288, cric-RNF13, has_cric_0004277, cric-ANRIL, cricuHRF1, has_cric_103047, *IL-6*, and *NF-κB* ($p = 0.0003$, $p = 0.0098$, $p = 0.009$, $p = 0.0136$, $p < 0.0001$, and $p = 0.0136$, respectively). However, has_cric_103047 and *IL-6* were not significant ($p = 0.3507$ and $p = 0.1639$, respectively). All cricRNAs and biomarkers showed sensitivity (ranging from 88.89% to 33.33%) and specificity (ranging from 90% to 42.11%) for the identification of G3 group. A combined cricRNA panel and biomarkers' overall sensitivity, specificity, and AUC were 80.42%, 56.64%, and 0.7470, respectively ($p < 0.0001$) (Supporting Information S1: Table S1).

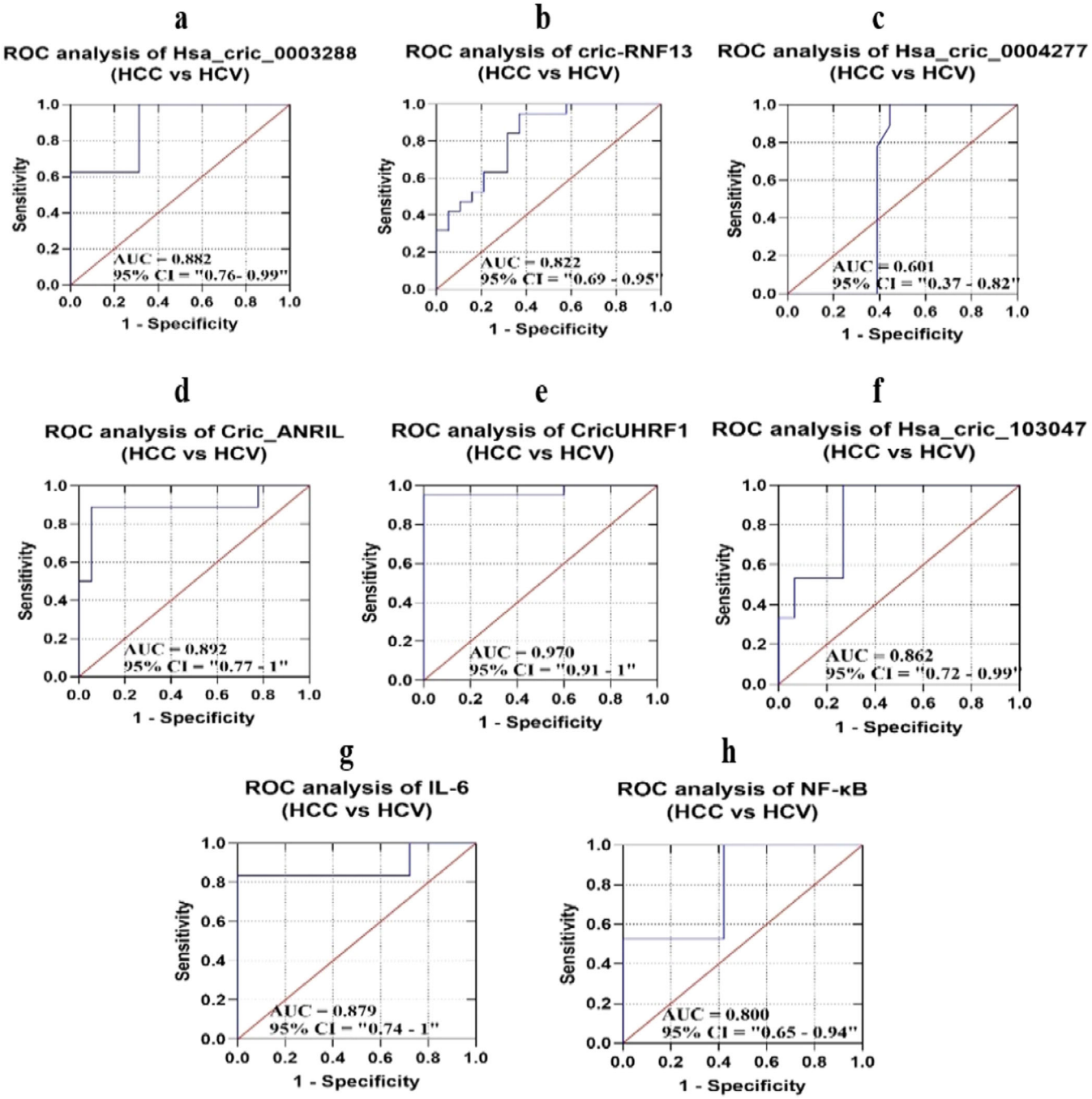

FIGURE 5 | ROC curves and AUC for cricRNAs and immune related biomarkers to distinguish the G2 group (HCC patients) from G1 group (HCV patients). The diagnostic potential and AUC of 6 cricRNAs and 2 biomarkers [(a) hsa_cric_0003288, (b) cric-RNF13, (c) hsa_cric_0004277, (d) cric-ANRIL, (e) cricuHRF1, (f) hsa_cric_103047, (g) IL-6, and (h) NF-κB] were estimated.

3.3.6 | Diagnostic Potential of CricRNAs and Biomarkers in G3 Group in Comparison With G2 Group

ROC curves were created for candidate cricRNAs and immune biomarkers to differentiate the G2 group from G2 group (Figure 8). AUC values were 0.5215, 0.5983, 0.5062, 0.608, 0.66, 0.6533, 0.6574, and 0.6302, corresponding to has_cric_0003288, cric-RNF13, has_cric_0004277, cric-ANRIL, cricuHRF1, has_cric_103047, *IL-6*, and *NF-κB*, respectively. The p-values were statistically significant only for cricuHRF1 ($p = 0.0834$). The *p*-values of has_cric_0003288, cric-RNF13, has_cric_0004277, cric-ANRIL, has_cric_103047, *IL-6*, and *NF-κB* were not significant. All cricRNAs and biomarkers showed sensitivity (ranging from 77.78% to 50%) and specificity (ranging from 94.4% to 38.89%) for the identification of G2 group. A combined cricRNA panel and biomarkers' overall sensitivity, specificity, and AUC were 50.35%, 65.03%, and 0.5991, respectively ($p = 0.0037$) (Supporting Information S1: Table S1).

3.4 | CircRNA–miRNA–mRNA Network Construction

To find out the possible miRNA and gene associations with has_cric_0003288, cric-RNF13, has_cric_0004277, cric-ANRIL,

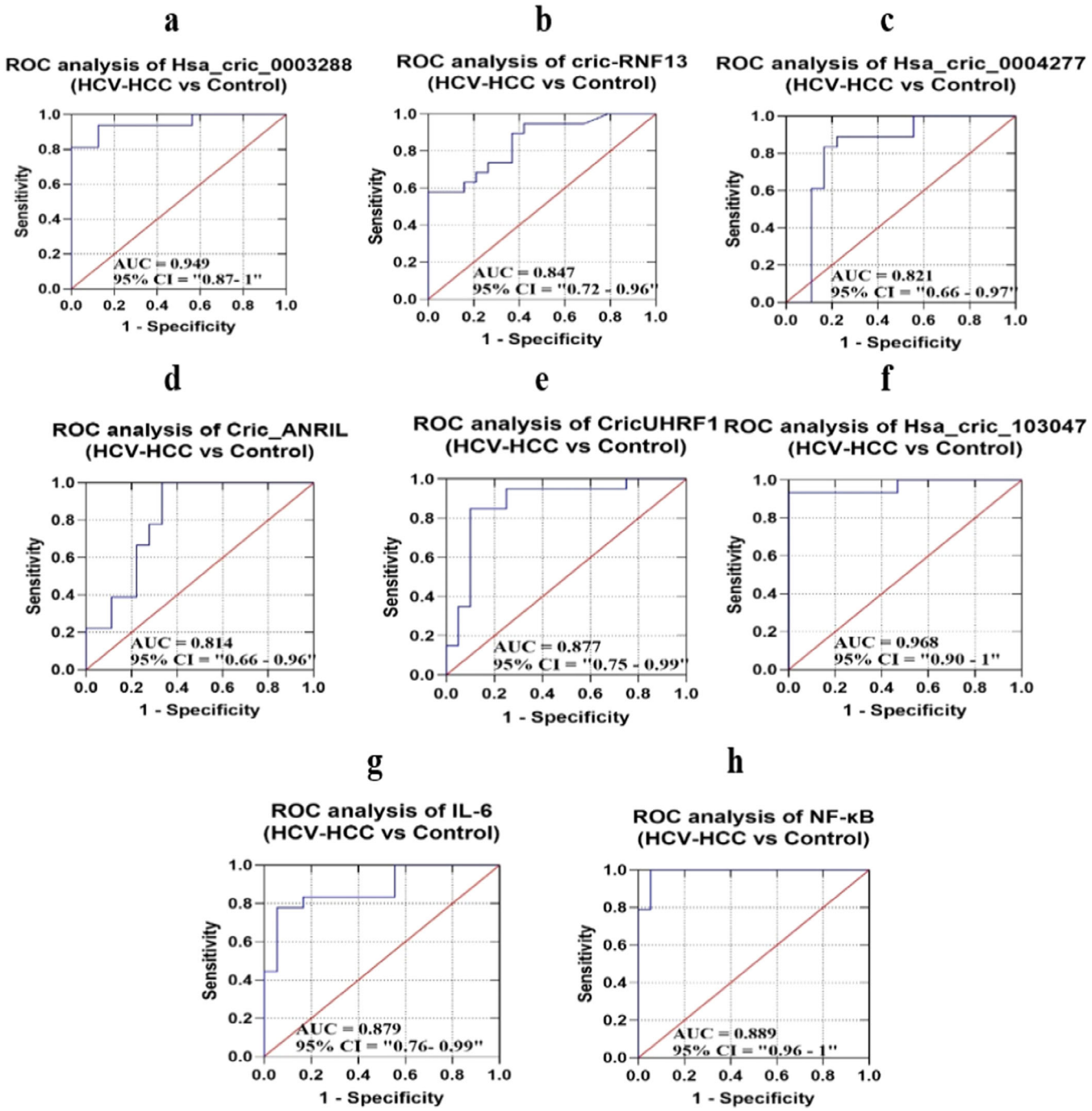

FIGURE 6 | ROC curves and AUC for cricRNAs and immune related biomarkers to discriminate the G3 group (HCV-HCC patients) from G0 group (normal controls). The diagnostic potential and AUC of 6 cricRNAs and 2 biomarkers [(a) hsa_cric_0003288, (b) cric-RNF13, (c) hsa_cric_0004277, (d) cric-ANRIL, (e) cricuHRF1, (f) hsa_cric_103047, (g) IL-6, and (h) NF-κB] were calculated.

cricuHRF1, and has_cric_103047, we used CircNetVis (https://www.meb.ki.se/shiny/truvu/CircNetVis/) [30]. The result implied that dozens of miRNAs can interact with has_cric_0003288, cric-RNF13, has_cric_0004277, cric-ANRIL, and cricuHRF1(Figure 9). We selected all possible miRNAs and found their target genes in each miRNA with the help of TargetScan [31]. Cytoscape (version 3.10.1) was used to construct the cricRNA-miRNA-mRNA network [32]. We can observe the potential target genes of has_cric_0003288, cric-RNF13, has_cric_0004277, cric-ANRIL, cricuHRF1, and has_cric_103047 (Figure 10).

4 | Discussion

HCV infection is a major risk factor for the development of HCC, one of the most common and deadly forms of liver cancer. Chronic HCV infection leads to persistent liver inflammation, which over time causes liver damage, fibrosis, and cirrhosis, significantly increasing the likelihood of HCC development [12, 16]. These noncoding RNAs act as "sponges" for microRNAs (miRNAs), preventing them from binding to their target mRNAs, which in turn modulates the expression of genes related to cancer progression [20].

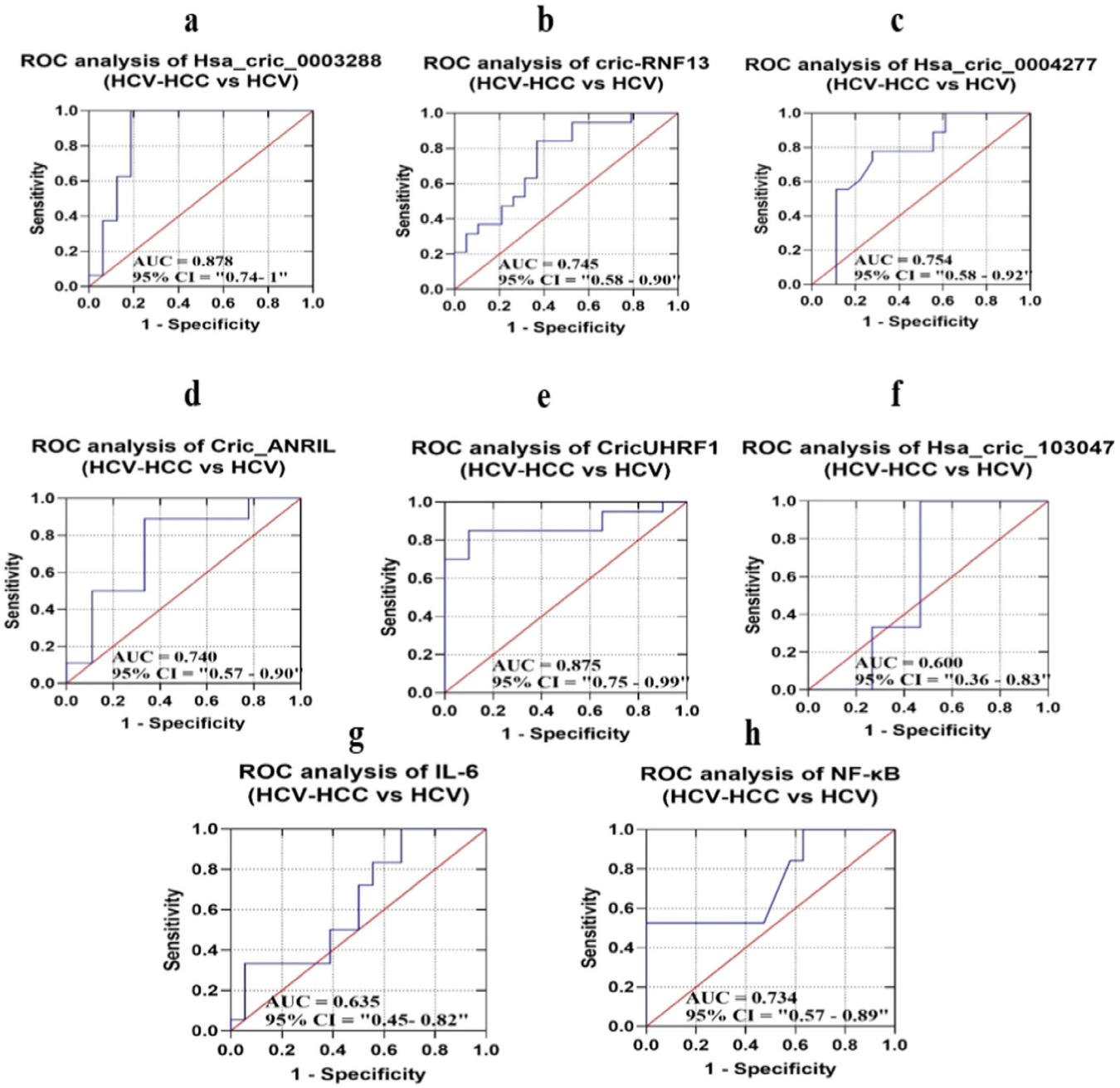

FIGURE 7 | ROC curves and AUC for cricRNAs and immune related biomarkers to discriminate the G3 group (HCC-HCC patients) from G1 group (HCV patients). The diagnostic potential and AUC of 6 cricRNAs and 2 biomarkers [(a) hsa_cric_0003288, (b) cric-RNF13, (c) hsa_cric_0004277, (d) cric-ANRIL, (e) cricuHRF1, (f) hsa_cric_103047, (g) IL-6, and (h) NF-κB] were calculated.

CircRNAs play a crucial role in the development of HCV-induced HCC by regulating various molecular pathways involved in liver tumorigenesis [20]. Given their stability in the bloodstream and disease-specific expression, circRNAs have the potential to serve as noninvasive biomarkers for early diagnosis, prognosis, and treatment monitoring in HCV-related HCC. However, their precise role and the mechanisms through which they contribute to HCV-induced HCC remain areas of ongoing research. Overall, studying circRNAs in this context holds great potential for improving both the understanding and clinical management of HCV-related liver cancer. Investigating these molecules could fill important knowledge gaps and provide new perspectives on how chronic HCV infection leads to liver cancer. circRNAs are expected to gain significant attention for their diagnostic and therapeutic potential, particularly in the context of diseases like HCC and other cancers.

CircRNAs indirectly influence antitumor immune responses [11] by affecting some protein stability; for instance, circ-Foxo3 and murine double minute 2 (MDM2) cause tumor protein p53 (Tp53) degradation, a key component of immune responses in tumorigenesis [34]. cricRNAs can also act as tumor antigens, regulating cell-to-cell communication between immunocytes and tumor cells [35]. KRAS-mutant colorectal cancer (CRC) cells transport various circRNAs into exosomes [36]. CricRNAs can bind with tumor-specific miRNAs and genes, forming a

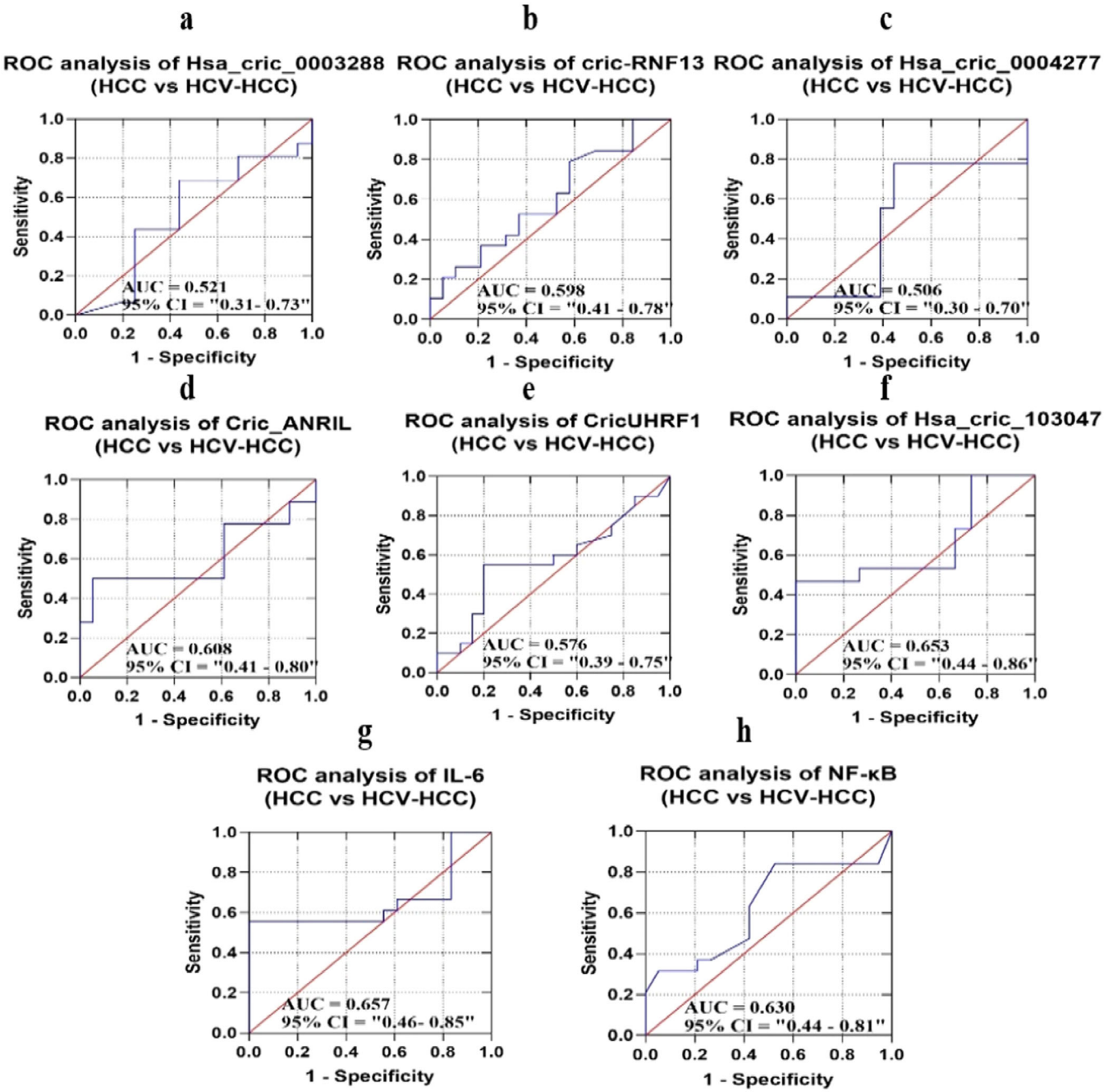

FIGURE 8 | ROC curves and AUC for cricRNAs and immune related biomarkers to differentiate the G2 group (HCC patients) from G3 group (HCV-HCC patients). The diagnostic potential and AUC of 6 cricRNAs and 2 biomarkers [(a) hsa_cric_0003288, (b) cric-RNF13, (c) hsa_cric_0004277, (d) cric-ANRIL, (e) cricuHRF1, (f) hsa_cric_103047, (g) IL-6, and (h) NF-κB] were calculated.

tumor antigen that enhances their stability and release [37]. Some circRNAs can activate immunocytes, promoting their fight against tumor. Recent studies show circRNAs can stimulate RIG-1 expression, triggering innate immune responses [18].

Ouyang et al. reported that has_cric_103047 high expression in peripheral blood mononuclear cells (PBMCs) and act as a promising diagnostic biomarker for rheumatoid arthritis [38]. In acute myeloid leukemia (AML), hsa_cric_0004277 expression was significantly downregulated and act as a promising diagnostic biomarker [39]. Xu et al. found that hsa_circ_0003288 regulates EMT and invasion of HCC by programmed death-1 ligand 1 (PD-L1) [40]. PD-L1 suppresses the immune response by preventing the proliferation of PD-1 positive cells, their cytokine secretion, and inducing apoptosis [41]. Hsa_circ_0003288 upregulates PD-L1 expression by sponge miR-145 via the PI3K/AKT signaling pathway [40]. Zhang et al. reported that circUHRF1 induces NK cell dysfunction, contributing to immunosuppression and resistance to anti-PD1 immunotherapy in HCC [25]. In the pancreatic cancer cell line, circRNF13 is high expressed, sponge miR-139-5p expression and act as an endogenous RNA of insulin-like growth factor I (IGF1R) [42]. IGF-1R is expressed in B [43] and T cells, offering a potential role in immune response regulation [44]. Holdt et al. found

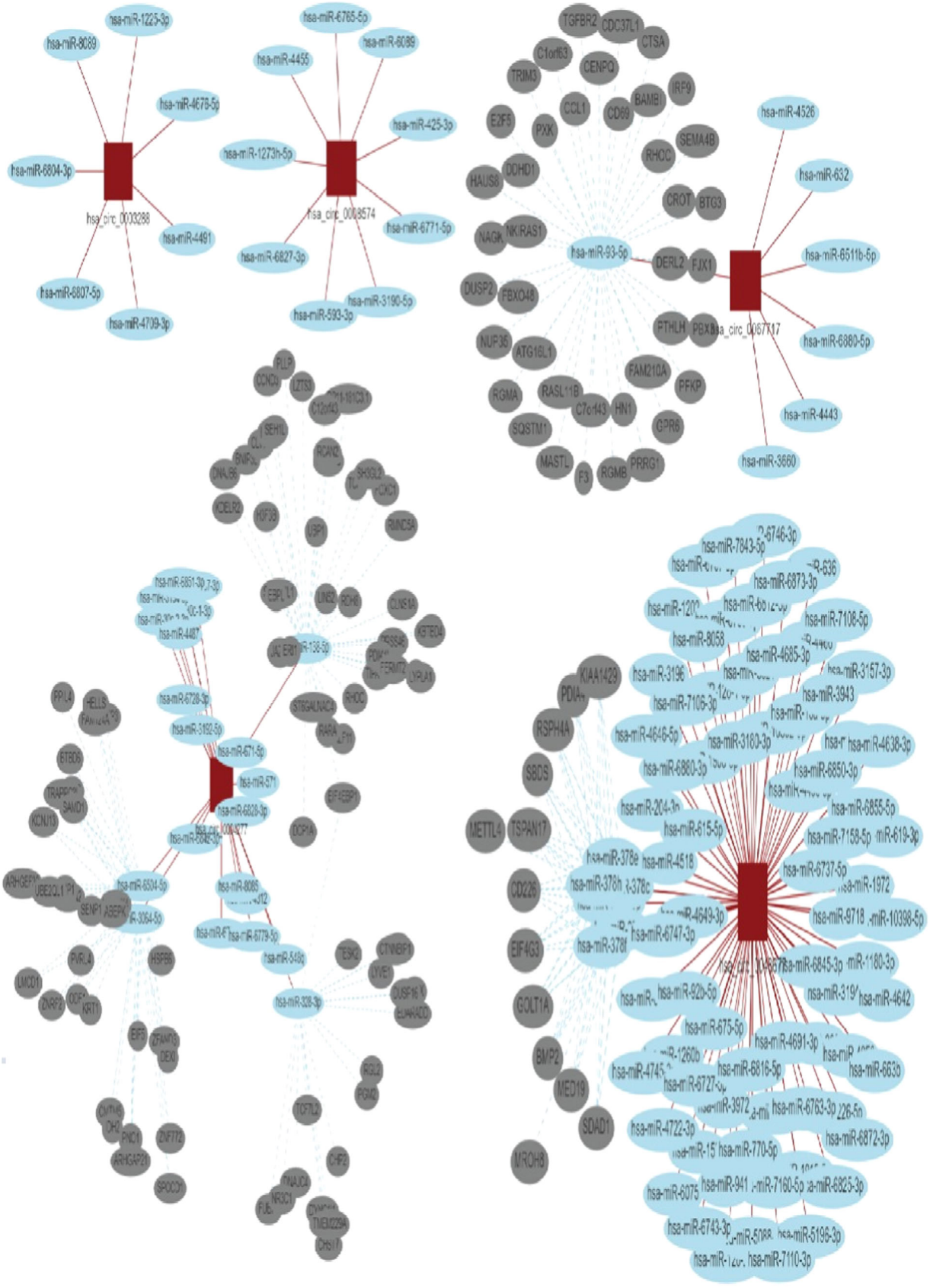

FIGURE 9 | CricRNA-miRNA-mRNA interaction network by CircNetVis. The red square shapes represented cricRNAs, the blue round shapes represented miRNAs, and the gray round shapes represented target mRNAs.

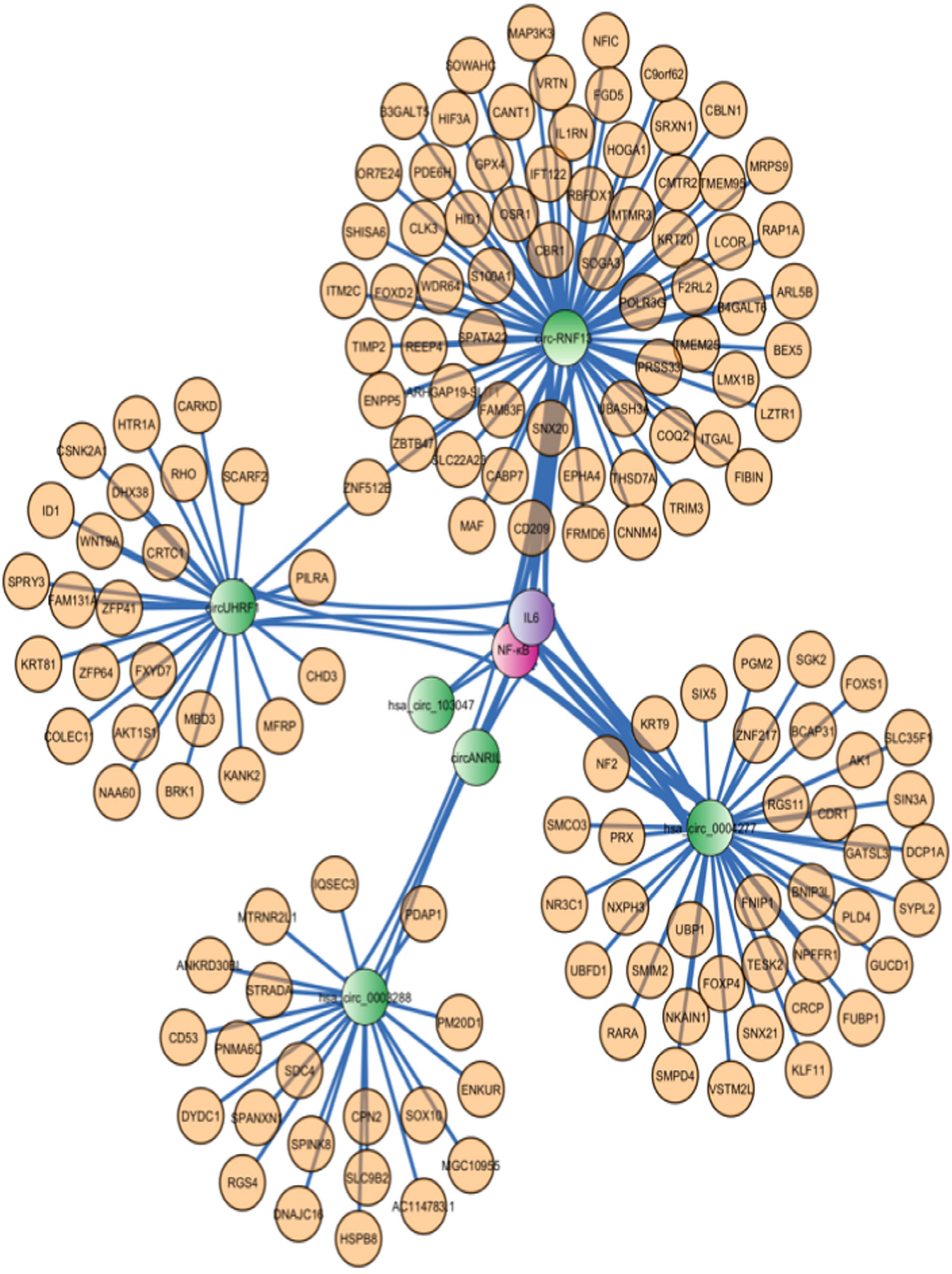

FIGURE 10 | CricRNAs and their possible target gene interaction construction by Cytoscape. The green one represented cricRNAs, the peach ones represented target genes, and pink and violet represented immune-related biomarkers NF-κB and IL-6, respectively.

that circ-ANRIL can inhibit pre-rRNA generation and ribosome formation in macrophages, induce apoptosis, and reduce proliferation via Tp53 expression [45]. When considered collectively, these data suggest that circRNAs are extensively expressed and have a variety of functions when it comes to regulating antitumor immune responses.

In the current study, data mining was conducted to identify immune-related circRNAs, including hsa_circ_0003288, circ-RNF13, hsa_circ_0004277, circANRIL, circUHRF1, and hsa_circ_103047, alongside immune-related biomarkers such as IL-6 and NF-κB. These circRNAs and biomarkers were selected to form a potential diagnostic panel for assessing their relevance in HCV-induced HCC. The goal was to explore their roles in immune regulation and evaluate their diagnostic utility in distinguishing between HCV patients (G1), HCC patients with unknown disease etiology (G2), HCC-induced HCC patients (G3) and healthy individuals (G0). RT-PCR was performed to check their expression in the G0, G1, G2, and G3 study groups. The expression levels of hsa_cric_0003288, cric-RNF13, hsa_cric_0004277, cric-ANRIL, cricuHRF1, hsa_cric_103047, and NF-κB were also significantly upregulated in G2 group ($p = 0.0056$, $p = 0.0255$, $p = 0.0072$, $p = 0.0050$, $p = 0.0171$, $p = 0.0096$, and $p = 0.0275$, respectively) and in G3 group ($p = 0.0308$, $p = 0.025$, $p = 0.0351$, $p = 0.0296$, $p = 0.0176$, $p = 0.0465$, and $p = 0.0408$, respectively) as compared with G1 group. However, no significant difference was found in the relative expression levels of hsa_cric_0003288, cric-RNF13, hsa_cric_0004277, cric-ANRIL, cricuHRF1, hsa_cric_103047, IL-6, and NF-κB among G1 and G0 groups, and as well as in G2 and G3 groups, as shown in Figure 2.

In addition, we observed that the expression of all cricRNAs including, hsa_cric_0003288, hsa_cric_0004277, cric-ANRIL, and cricUHRF1, was not correlated with IL-6 and NF-κB, indicating these circRNAs may not be relevant to these immune-related biomarkers in G1 and G2 groups. However, we found that the expression level of 2 cricRNAs was correlated with these immune-related biomarkers; for example, cric-RNF13 ($r = -0.5352$, $p < 0.0221$) was negatively correlated only with IL-6 and hsa_cric_103047 ($r = -0.5865$, $p < 0.0240$) was negatively correlated only with NF-κB in G3 group, as mentioned in Table 2. Therefore, we speculate that directly or indirectly, these cricRNAs may interact with each other; however, there is a need for further experimentation to check this possibility.

Furthermore, our analysis revealed that hsa_cric_0003288 (AUC = 0.9609), hsa_cric_103047 (AUC = 0.9822), cric_RNF13 (AUC = 0.892), cric-ANRIL (AUC = 0.9815) and cricUHRF1 (AUC = 0.945) for G2 group and hsa_cric_0003288 (AUC = 0.9492), hsa_cric_0004277 (AUC = 0.821) and hsa_cric_103047 (AUC = 0.9689) have diagnostic potential values for G3 group, as mentioned in Supporting Information S1: Table S1. This was especially true in the case of hsa_cric_0003288, hsa_cric_103047, cric-ANRIL, and cricUHRF1, which had significant ROC AUC values, indicating that they have great potential as diagnostic biomarkers.

We found that hsa_cric_0003288, hsa_cric_0004277, and hsa_cric_103047 have diagnostic potential values for G3 group (HCV-HCC detection), and this cricRNA panel may serve as diagnostic biomarkers in the future. However, there are some limitations in this study, like the relatively small sample size; the data may be confirmed by a population-based study; and there is a need for further experimentation to evaluate the ability of the above circRNA panel to effectively discriminate HCV-HCC from other malignancies.

5 | Conclusions

The data of the current study revealed that immune-related cricRNAs, including hsa_circ_0003288, circ-RNF13, circANRIL, circUHRF1, and hsa_circ_103047, could serve as diagnostic biomarkers and therapeutic targets for HCV-induced HCC.

Author Contributions

Yasmeen Ishaq: conceptualization, data curation, formal analysis, investigation, methodology, software, validation, visualization, writing–original draft, writing–review and editing. **Bisma Rauff:** formal analysis, writing–review and editing. **Badr Alzahrani:** formal analysis, funding acquisition, writing–review and editing. **Hassnain Javed:** methodology, resources, supervision, writing–review and editing. **Aqsa Ikram:** conceptualization, funding acquisition, project administration, resources, supervision, writing–review and editing.

Acknowledgments

The authors would like to acknowledge the Institute of Molecular Biology and Biotechnology, University of Lahore, Pakistan. The authors would also like to acknowledge the Deputyship for Research & Innovation, Ministry of Education in Saudi Arabia for funding this research through project number 223202. The funding Sources helps in study design; collection, analysis, and interpretation of data.

Ethics Statement

Approval of the research protocol by an Institutional Reviewer Board: The present research was approved by the Ethical Committee of the Institute of Molecular Biology and Biotechnology (IMBB), University of Lahore, Lahore Pakistan.

Conflicts of Interest

All the authors have no conflicts of interest in this study. All authors have read and approved the final version of the manuscript and corresponding author AI had full access to all of the data in this study and takes complete responsibility for the integrity of the data and the accuracy of the data analysis.

Data Availability Statement

Research data are not shared. it can be shared upon suitable request.

References

1. T. K. Sahin, A. Rizzo, S. Aksoy, and D. C. Guven, "Prognostic Significance of the Royal Marsden Hospital (RMH) Score in Patients With Cancer: A Systematic Review and Meta-Analysis," *Cancers* 16, no. 10 (2024): 1835.

2. Y. Ishaq, A. Ikram, B. Alzahrani, and S. Khurshid, "The Role of miRNAs, circRNAs and Their Interactions in Development and Progression of Hepatocellular Carcinoma: An Insilico Approach," *Genes* 14, no. 1 (2023): 13.

3. A. Rizzo and A. D. Ricci, "Challenges and Future Trends of Hepatocellular Carcinoma Immunotherapy," *International Journal of Molecular Sciences* 23 (2022): 11363.

4. A. Rizzo, M. Santoni, V. Mollica, et al., "Peripheral Neuropathy and Headache in Cancer Patients Treated With Immunotherapy and Immuno-Oncology Combinations: The MOUSEION-02 Study," *Expert Opinion on Drug Metabolism & Toxicology* 17, no. 12 (2021): 1455–1466.

5. H. Alotaibi, "Molecular Mechanisms of Hepatocellular Carcinoma." *in* Hepatocellular Carcinoma (Springer, 2016), 43–63.

6. T. L. Laursen, T. D. Sandahl, K. Kazankov, J. George, and H. Grønbæk, "Liver-Related Effects of Chronic Hepatitis C Antiviral Treatment," *World Journal of Gastroenterology* 26, no. 22 (2020): 2931–2947.

7. A. Rizzo, A. D. Ricci, and G. Brandi, "Trans-Arterial Chemoembolization Plus Systemic Treatments for Hepatocellular Carcinoma: An Update," *Journal of Personalized Medicine* 12, no. 11 (2022): 1788.

8. J. Grebely, G. J. Dore, A. Y. Kim, et al., "Genetics of Spontaneous Clearance of Hepatitis C Virus Infection: A Complex Topic With Much to Learn," *Hepatology (Baltimore, Md.)* 60, no. 6 (2014): 2127–2128.

9. P. Tandon, *Clinical Decision Support System for the Diagnosis, Analysis and Management of Hepatitis C*, Rutgers The State University of New Jersey, Rutgers School of Health Professions, 2020.

10. X. Li, L. Wang, and P. Gao, "Chronic Hepatitis C Virus Infection: Relationships Between Inflammatory Marker Levels and Compensated Liver Cirrhosis," *Medicine* 98, no. 39 (2019): e17300.

11. D. C. Guven, E. Erul, Y. Kaygusuz, et al., "Immune Checkpoint Inhibitor-Related Hearing Loss: A Systematic Review and Analysis of Individual Patient Data," *Supportive Care in Cancer* 31, no. 11 (2023): 624.

12. Q. Li, Y. Tian, Y. Liang, and C. Li, "CircHIPK3/miR-876-5p/PIK3R1 Axis Regulates Regulation Proliferation, Migration, Invasion, and Glutaminolysis in Gastric Cancer Cells," *Cancer Cell International* 20, no. 1 (2020): 391.

13. W. Jiang, "Circ-ATP5H Induces Hepatitis B Virus Replication and Expression By Regulating miR-138-5p/TNFAIP3 Axis," *Cancer Management and Research* 12 (2020): 11031–11040.

14. D. Xiong, Y. Dang, P. Lin, et al., "A CircRNA–miRNA–mRNA Network Identification for Exploring Underlying Pathogenesis and Therapy Strategy of Hepatocellular Carcinoma," *Journal of Translational Medicine* 16 (2018): 220.

15. M. Wang, F. Yu, and P. Li, "Circular RNAs: Characteristics, Function and Clinical Significance in Hepatocellular Carcinoma," *Cancers* 10, no. 8 (2018): 258.

16. L. Guan, Q. Hao, F. Shi, et al., "Regulation of the Tumor Immune Microenvironment by Cancer-Derived Circular Rnas," *Cell Death & Disease* 14, no. 2 (2023): 132.

17. X. Chen, T. Yang, W. Wang, et al., "Circular RNAs in Immune Responses and Immune Diseases," *Theranostics* 9, no. 2 (2019): 588–607.

18. C. Cadena and S. Hur, "Antiviral Immunity and Circular RNA: No End in Sight," *Molecular Cell* 67, no. 2 (2017): 163–164.

19. M. Pu, J. Chen, Z. Tao, et al., "Regulatory Network of miRNA on Its Target: Coordination Between Transcriptional and Post-Transcriptional Regulation of Gene Expression," *Cellular and Molecular Life Sciences* 76 (2019): 441–451.

20. T. Abaza, M. K. A. El-Aziz, K. A. Daniel, et al., "Emerging Role of Circular RNAs in Hepatocellular Carcinoma Immunotherapy," *International Journal of Molecular Sciences* 24, no. 22 (2023): 16484.

21. G. Xu, P. Zhang, H. Liang, et al., "Circular RNA hsa_circ_0003288 Induces EMT and Invasion by Regulating hsa_circ_0003288/miR-145/PD-L1 Axis in Hepatocellular Carcinoma," *Cancer Cell International* 21 (2021): 212.

22. J. Shi, X. Rui, C. Han, C. Wang, L. Xu, and X. Jiang, "circRNF13, a Novel N6-methyladenosine-modified Circular RNA, Enhances Radioresistance in Cervical Cancer by Increasing CXCL1 Mrna Stability," *Cell Death Discovery* 9, no. 1 (2023): 253.

23. L. Yang, "Circular RNA hsa_circ_0004277 Contributes to Malignant Phenotype of Colorectal Cancer by Sponging miR-512-5p to Upregulate the Expression of PTMA," *Journal of Cellular Physiology* 59 (2020): 88.

24. Q. Qin, P. Zheng, R. Tu, J. Huang, and X. Cao, "Integrated Bioinformatics Analysis for the Identification of Hub Genes and Signaling Pathways Related to Circanril," *PeerJ* 10 (2022): e13135.

25. P.-F. Zhang, C. Gao, X. Y. Huang, et al., "Cancer Cell-Derived Exosomal circUHRF1 Induces Natural Killer Cell Exhaustion and May Cause Resistance to anti-PD1 Therapy in Hepatocellular Carcinoma," *Molecular Cancer* 19 (2020): 110.

26. Q. Luo, L. Zeng, L. Zeng, et al., "Expression and Clinical Significance of Circular RNAs hsa_circ_0000175 and hsa_circ_0008410 in Peripheral Blood Mononuclear Cells From Patients With Rheumatoid Arthritis," *International Journal of Molecular Medicine* 45, no. 4 (2020): 1203–1212.

27. M. Assel, D. Sjoberg, A. Elders, et al., "Guidelines for Reporting of Statistics for Clinical Research in Urology," *Journal of Urology* 201, no. 3 (2019): 595–604.

28. J. A. Bennett, "The Consolidated Standards of Reporting Trials (Consort): Guidelines for Reporting Randomized Trials," *Nursing Research* 54, no. 2 (2005): 128–132.

29. K. J. Livak and T. D. Schmittgen, "Analysis of Relative Gene Expression Data Using Real-Time Quantitative Pcr and the 2(-Delta Delta C(T)) Method," *Methods (San Diego, Calif.)* 25, no. 4 (2001): 402–408.

30. T.-H. Nguyen, H.-N. Nguyen, and T. N. Vu, "Circnetvis: an Interactive Web Application for Visualizing Interaction Networks of Circular RNAs," *BMC Bioinformatics* 25, no. 1 (2024): 31.

31. B. Edris, "A comparison of the Oligomap and TargetScan algorithms for miRNA target analysis." *Bmi* (stanford. edu, 2011). 231.

32. N. Oktaviana, A. H. Lutfitasari, and W. A. Kusuma, "Exploring Malaria Disease Biomarkers: An Integrated Approach Using Network Topology And Enrichment Analysis," *Indian Journal of Computer Science and Engineering* 15 (2024): 88–96.

33. T. A. Lang and D. G. Altman, "Statistical Analyses and Methods in the Published Literature: The Sampl Guidelines," *Guidelines For Reporting Health Research: A User's Manual* 25 (2014): 264–274.

34. E. Farhadi, M. Khomeijani-Farahani, R. Nikbakhsh, et al., "The Potential Role of Circular Rnas in Regulating p53 in Different Types of Cancers," *Pathology - Research and Practice* 261 (2024): 155488.

35. Y. Dou, D. J. Cha, J. L. Franklin, et al., "Circular Rnas Are Down-Regulated in Kras Mutant Colon Cancer Cells and Can Be Transferred to Exosomes," *Scientific Reports* 6, no. 1 (2016): 37982.

36. F. Vakhshiteh, S. Hassani, N. Momenifar, and F. Pakdaman, "Exosomal Circrnas: New Players in Colorectal Cancer," *Cancer Cell International* 21, no. 1 (2021): 483.

37. Z. Xu, P. Li, L. Fan, and M. Wu, "The Potential Role of Circrna in Tumor Immunity Regulation and Immunotherapy," *Frontiers in Immunology* 9 (2018): 2018.

38. Q. Ouyang, J. Wu, Z. Jiang, et al., "Microarray Expression Profile of circular RNAs in Peripheral Blood Mononuclear Cells from Rheumatoid Arthritis Patients," *Cellular Physiology and Biochemistry* 42, no. 2 (2017): 651–659.

39. W. Li, C. Zhong, J. Jiao, et al., "Characterization of hsa_-circ_0004277 as a New Biomarker for Acute Myeloid Leukemia via

Circular Rna Profile and Bioinformatics Analysis," *International Journal of Molecular Sciences* 18, no. 3 (2017): 597.

40. G. Xu, P. Zhang, H. Liang, et al., "Circular RNA hsa_circ_0003288 Induces Emt and Invasion By Regulating hsa_circ_0003288/miR-145/PD-L1 Axis in Hepatocellular Carcinoma," *Cancer Cell International* 21, no. 1 (2021): 212.

41. Y. Han, D. Liu, and L. Li, "PD-1/PD-L1 Pathway: Current Researches in Cancer," *American Journal of Cancer Research* 10, no. 3 (2020): 727–742.

42. X. Liu, L. Zhou, Y. Chen, X. Jiang, and J. Jiang, "CircRNF13 Promotes the Malignant Progression of Pancreatic Cancer through Targeting miR-139-5p/IGF1R Axis," *Journal of Oncology* 2021 (2021): 1–15.

43. R. Wang, D. Song, Y. Zhong, and H. Li, "Potential Role of IGF-1R in the Interaction Between Orbital Fibroblasts and B Lymphocytes: An Implication for B Lymphocyte Depletion in the Active Inflammatory Phase of Thyroid-Associated Ophthalmopathy," *BMC Immunology* 25, no. 1 (2024): 31.

44. D. DiToro, S. N. Harbour, J. K. Bando, et al., "Insulin-Like Growth Factors Are Key Regulators of T Helper 17 Regulatory T Cell Balance in Autoimmunity," *Immunity* 52, no. 4 (2020): 650–667.e10.

45. L. M. Holdt, A. Stahringer, K. Sass, et al., "Circular Non-Coding RNA Anril Modulates Ribosomal RNA Maturation and Atherosclerosis in Humans," *Nature Communications* 7, no. 1 (2016): 12429.

Supporting Information

Additional supporting information can be found online in the Supporting Information section.